To appear in: "Advanced Solar Polarimetry – Theory, Observation, and Instrumentation", Ed. M. Sigwarth, Procs. "20th NSO/SP Summer Workshop", Astron. Soc. Pac. Conf. Series, in press. Preprint: http://www.astro.uu.nl/~rutten/

Proxy magnetometry of the photosphere: why are G-band bright points so bright?

Robert J. Rutten

Sterrekundig Instituut, Postbus 80 000, NL–3508 TA Utrecht, The Netherlands

Dan Kiselman, Luc Rouppe van der Voort

The Royal Swedish Academy of Sciences, Stockholm Observatory, SE–133 36 Saltsjöbaden, Sweden

Bertrand Plez

GRAAL, Université de Montpellier II, FR–34095 Montpellier Cedex 5, France

Abstract. We discuss the formation of G-band bright points in terms of standard fluxtube modeling, in particular the 1D LTE models constructed by Solanki and coworkers. Combined with LTE spectral synthesis they explain observed G-band bright point contrasts quite well. The G-band contrast increase over the continuum is due to the enhancement of the hot-wall effect by CH depletion within the fluxtube. The modeling predicts that the CN band at 388 nm shows magnetic elements at yet higher contrast, which was tested using the last light of the Swedish Vacuum Solar Telescope on La Palma. The issue whether the standard fluxtube models have erroneous temperature stratifications due to neglect of NLTE irradiation remains open. It is important because the stratifications imply considerable heating.

1. G-band bright points

The roughly 1 nm wide band with CH lines around $\lambda = 430.5$ nm which Fraunhofer (1817) labeled G in his initial inventory of the visible solar spectrum has emerged as the principal diagnostic to study photospheric magnetism at the highest achievable angular resolution. Richard Muller was the pioneer[1], using the sometimes near-perfect seeing at Pic du Midi to produce the first image sequences displaying magnetic elements as bright points (Muller et al. 1989, Auffret & Muller 1991, Muller & Roudier 1992, Muller 1994, Dermendjev et al.

[1]He reports that the G-band story began by his noting it as a particularly dark feature on a print of the solar spectrum adorning Serge Koutchmy's office. He has often denoted the G-band as due to CN but the lines are from CH.

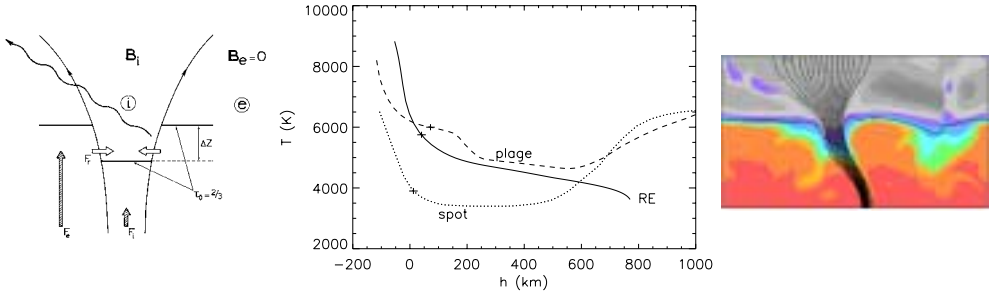

Figure 1. Fluxtube modeling at different levels of sophistication. Left: magnetostatic paradigm, from Schrijver & Zwaan (2000). Middle: standard models, from Stuik et al. (1997). The plage model describes fluxtubes at 15% filling factor and comes from Bruls & Solanki (1993), the RE model describes an Uppsala radiative equilibrium stratification for the sun ($T_{\rm eff}$ = 5750 K), the sunspot model is from Maltby et al. (1986). Each model is shown on its own height scale having $\tau = 1$ at $h = 0$ km; the plage fluxtube model has a Wilson depression (shift to the left) of 185 km and reaches $B = 2200$ G at $h = 0$ km. The crosses mark the effective temperatures. Right: numerical fluxsheet simulation, from http://www.kis.uni-freiburg.de/∼steiner.

1994, Muller & Roudier 1994, Muller et al. 1994, Roudier et al. 1994, Moity et al. 1999). The late Swedish Vacuum Solar Telescope (SVST) then took over, particularly in the hands of the Lockheed group using the Stockholm phase diversity technique for image restoration (Berger et al. 1995, Berger & Title 1996, Title & Berger 1996, Löfdahl & Scharmer 1994, Löfdahl et al. 1998, Berger et al. 1998b, Berger et al. 1998a). At present, the Dutch Open Telescope (DOT) takes over the role of high-resolution G-band imager from the SVST from whose building it is operated. The DOT concept and speckle restoration are described elsewhere in these proceedings while DOT G-band movies are available at http://dot.astro.uu.nl and vividly demonstrate the capability that the G band offers to locate and track minute magnetic elements in the solar photosphere by portraying these as bright points ("proxy magnetometry").

2. Fluxtube models

Figure 1 illustrates three levels of sophistication in modeling magnetic elements in the solar photosphere. Modelers call these elements "fluxtubes".

The concept (left) came from Kees Zwaan. It was (as happened so often with Zwaan's ideas) thoroughly worked out in the Zwaan-supervised thesis of Spruit (1977) and followed by the fluxtube collapse scenario (Spruit 1979) and observational verification of the hot-wall effect (Spruit & Zwaan 1981). A still authorative summary is found in Spruit (1981); a newer one in Chapter 4 of Schrijver & Zwaan (2000). The cartoon at left is taken from the latter and describes the magnetostatic fluxtube. The magnetic pressure causes reduction of the gas pressure inside to balance the outside gas pressure at all heights. The tube expands with height due to the exponential pressure drop-off. The lower

gas pressure makes the tube relatively transparent so that the photon escape height (here at $\tau = 2/3$ for plane-parallel net radiative flux) is lowered over the Wilson depression. The horizontal arrows denote sideways irradiation by the walls which are hotter than the inside gas at given height due to a deficit in convective energy flux inside (vertical arrows). The hot walls make the tubes bright in oblique viewing. At disk center a line of sight along the tube axis may sample hotter or cooler gas than outside depending on the internal temperature stratification, but at less than perfect resolution the bright ring constituted by the sub-surface walls makes the unresolved fluxtube appear bright.

The standard fluxtube models come from Solanki with coworkers (e.g., Solanki & Stenflo 1985, Solanki 1986, Solanki et al. 1991, Solanki & Brigljevic 1992, Bünte et al. 1993, Bruls & Solanki 1993, Briand & Solanki 1995). The "plage" fluxtube model in the center plot of Fig. 1 is an example. It describes the temperature stratification along the axis of a magnetostatic fluxtube as constrained by a large assembly of spectral line observations, especially Stokes V profiles of Fe I lines measured with the Fourier Transform Spectrometer at the McMath-Pierce telescope at Kitt Peak. These data have bad angular resolution but superb spectral resolution and deliver empirical best-fit fluxtube models on the assumption that the spatially averaged Stokes V encoding by fluxtube interiors can be characterized by a single mean stratification plus a mean fluxtube shape. The latter is set magnetostatically as a function of spatial fluxtube density ("filling factor") meaning that the next same-polarity fluxtube is close enough to bend the field lines back to vertical at a certain distance from tube center. For the plage fluxtube model shown here this merging height with the next tube ("magnetic canopy") is at 360 km.

A more recent approach in such empirical modeling is to fit observations not by hand in a trial-and-error procedure but with the automated inversion technique developed at the IAC (Ruiz Cobo & Del Toro Iniesta 1992). The results on Solanki-like Stokes V input data with Solanki-like assumptions (1D stratification, magnetostatic fluxtube shape, LTE line formation) indeed recovers Solanki-like models (Bellot Rubio et al. 1998). Inversion techniques are extensively discussed elsewhere in these proceedings.

The state of the art is shown at right in Fig. 1 in the form of a snapshot from one of the numerical simulations by Steiner and coworkers (e.g., Steiner et al. 1998, Grossmann-Doerth et al. 1998, Steiner, these proceedings). These time-dependent MHD simulations come a long way in reproducing magnetic element observables (Leka et al. 1999), but by being 2D they lack the 3D instabilities that may disintegrate (or integrate) fluxtubes akin to the rapid changes that G-band bright points show, and the radiative transfer is severely simplified.

3. Fluxtube irradiation

Figure 2 is a cartoon in which the fluxtube width varies from wider than the internal mean free photon path to much thinner than that. The lefthand tube has small radiative exchange between outside and inside and so characterizes basic assumptions of Solanki-type modeling: lateral homogeneity in the tube and LTE line formation with 1D evaluation of the LTE source function along lines of sight that may cut through the wall into the underlying ambient atmosphere.

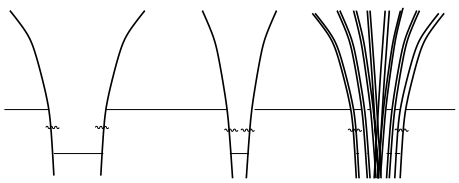

Figure 2. Schematic fluxtubes. Left: wide tube in which hot-wall radiation does not penetrate far. The temperature stratification should follow radiative equilibrium as in a plane-parallel atmosphere unless there is mechanical energy dissipation. The shallow gradients of the standard models imply considerable heating. Middle: narrow tube in which the hot-wall radiation may upset ionization (and possibly dissociation) equilibria as proposed by Rutten (1999). Right: microstructured fluxtube as proposed by Sánchez Almeida et al. (1996), consisting of an assembly of numerous very thin fluxtubes that share temperature with the ambient temperature through radiative exchange.

In this case one would expect a radiative equilibrium stratification unless there is non-radiative heating or cooling, and therefore one would expect that the plage model in Fig. 1 should correspond to a plane-parallel RE atmosphere at $T_{\rm eff} = 6100$ K — but it actually has a much flatter gradient at the depth where the bulk of the flux escapes (cross), implying much energy dissipation. The unknown dissipation mechanism must differ from processes that occur in the far larger "fluxtubes" represented by sunspot umbrae since the empirical sunspot model in Fig. 1 is close to radiative equilibrium (cf. Stuik et al. 1997).

The tube in the middle suffers from hot-wall irradiation of the tube interior. Rutten (1999) has argued that such irradiation may cause the flat gradient in the Solanki-type models (including the IAC Stokes inversions) through its neglect in neutral-metal ionization equilibria. The Fe I line weakening that actually results from irradiative overionization may be erroneously modeled as a too shallow source function gradient even while the actual temperature gradient follows radiative equilibrium. The corollary was that the G band might gain bright-point contrast from similar irradiative overdissociation of CH (Rutten 1999), but the molecular radiative rates may be too slow for that (Uitenbroek, private communication at this meeting).

The magnetic element at right consists of a cluster of very thin tubes rather than a monolithic one. This scheme follows the MISMA hypothesis (Sánchez Almeida et al. 1996, Sánchez Almeida 1997, Sánchez Almeida & Lites 2000) which implements the warnings of van Ballegooijen (1985) about the limited visibility of thin (and slanted) fluxtubes in Stokes data. In this case the optical transparency of the thin tubes implies efficient radiative exchange, so that they should share the ambient temperature at all heights (Jorge Sánchez, private communication). Radiative equilibrium would then establish a common gradient for the whole cluster with the tubes acting as photon leaks.

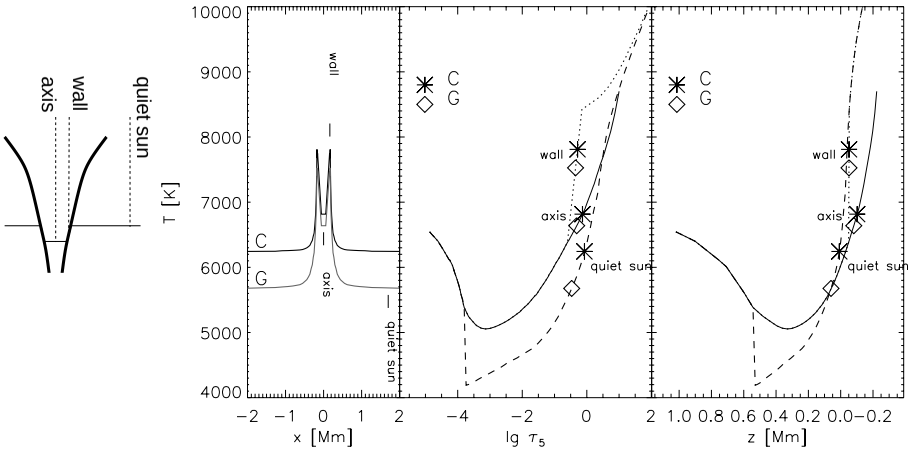

Figure 3. G band formation in standard LTE modelling. The sketch at left defines the three lines of sight for which the temperature stratifications are plotted at right, respectively against optical depth along the line of sight and against geometrical height. The symbols mark $\tau=1$ sampling heights, respectively for the G band (G) and for nearby continuum (C). The emergent brightness profiles across the fluxtube in the first panel are shown as brightness temperature so that each sample corresponds horizontally to formation temperature at right.

4. G-band contrast from standard modeling

We have performed detailed spectral line synthesis of the G band using "network" fluxtube model NCHROM7 of Briand & Solanki (1995), multi-ray 1D spectrum formation as in Fig. 2 of Solanki et al. (1991), and LTE excitation and ionization. The ambient mean photosphere is given by the HSRASP model of Spruit (1974) with a patched-on chromosphere that is not important here. The G band is synthesized in detail and then multiplied by a 1 nm FWHM Gaussian around $\lambda = 430.5$ nm to mimic filter observations.

Results are shown in Fig. 3. The NCHROM7 model (solid curves) does not have the distinct hump of the plage model in Fig. 1, but it does feature a markedly shallower temperature gradient than the HSRASP which again implies a large non-radiative source of energy that is dissipated much deeper than assumed in most MHD network heating mechanisms. The $\tau=1$ marks demonstrate that the bright peaks come from the hot walls: the dashed stratifications sample much higher temperature than the quiet-sun line of sight by having $\tau=1$ well below the outside surface. Thus, fluxtubes are like viewing pipes through which one observes hot subsurface layers. Note that in this model the fluxtube bottom is also hotter and brighter than the mean surface, so that a radiative-equilibrium fluxtube stratification would produce a hotter main-sequence spectrum ($T_{\rm eff} \approx 6300$ K) along the tube axis than the mean quiet sun.

The brightness profiles in the first panel of Figure 3 illustrate that the fluxtube contrast is larger in the G band. In the ambient quiet sun the G band is darker than the nearby continuum due to the many CH lines. The mean $\tau = 1$ escape depth is only slightly higher (righthand panel) so that G-band granulation looks the same as continuum granulation, as indeed observed. The hot-wall peaks darken less from C to G due to CH dissociation within the tube. Simply put, the CH lines go away so that the viewing pipe gets yet more transparent. Detailed analysis of the molecular equilibria in the fluxtube (which we aim to publish in a more comprehensive paper) shows that the very low CH dissociation energy and the very large hydrogen density combine to make the CH concentration peak in deep layers and vanish abruptly above the fluxtube wall. Thus, fluxtubes are bright in the G band not because the CH lines cause higher formation but because their disappearance causes relatively deep hot-wall viewing.

We have compared the computed fluxtube contrast with the ambient quiet sun with observations taken with the SVST by Löfdahl and Berger (private communication). Of course, even the SVST at the best La Palma seeing was not sharp enough to image solar fluxtubes as the tiny bright rings with less bright cores that the first panel of Fig. 3 predicts. An unknown amount of smearing by seeing and telescope imperfections must be added to the diffraction pattern set by the 47.5-cm aperture (0.2 arcsec resolution). We therefore compared the observed contrast enhancement between G band and nearby continuum in bright points with the computed enhancement applying reasonable smearing functions. The results have been shown elsewhere (Kiselman et al. 2001) and show good agreement within the uncertainties.

5. CN band as bright-point diagnostic

As part of our spectrum synthesis from the NCHROM7 fluxtube model we also assessed other parts of the spectrum. Results are shown in Fig. 3 of Kiselman et al. (2001) and indicate that another molecular band should provide even larger contrast enhancement, namely the CN band shortwards of $\lambda = 388$ nm. The computed contrast is about 40% larger than for the G-band for 1 nm filters. Some of the last light of the SVST (presently being rebuilt into the New Swedish Solar Telescope, see http://www.astro.su.se/groups/solar/NSST) was used to test this wavelength band as fluxtube diagnostic. A sample result in Fig. 4 illustrates that, apart from loss of resolution due to longer exposure, the CN band shows granulation and magnetic elements very much like the G band[2].

[2]The solar scene looks quite different in the CN spectroheliogram published by Liu & Sheeley (1971) but that was narrow-band at bandhead. It shows bright points in internetwork areas which Rutten & Uitenbroek (1991) interpreted as acoustic oscillation grains akin to the propagative whiskers in the inner wings of Ca II H & K.

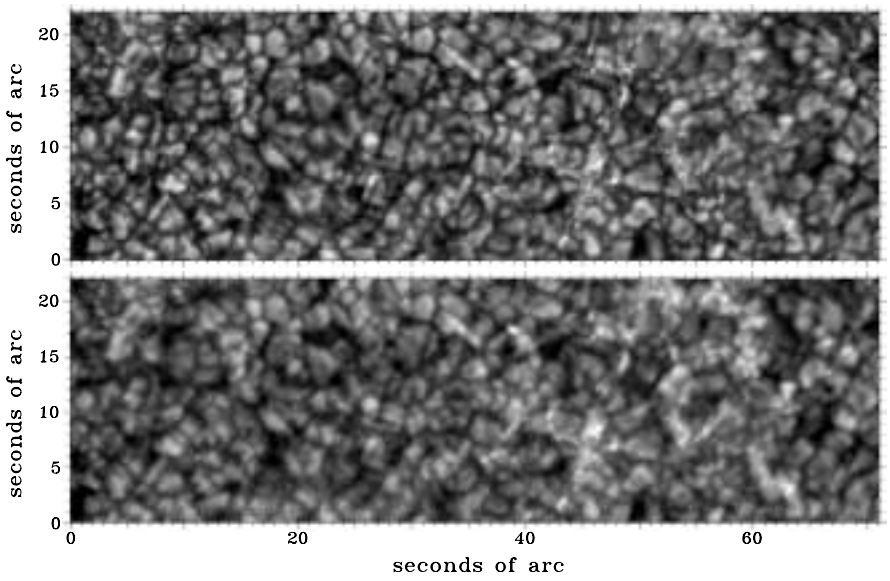

Figure 4. Small cutouts of two filtergrams taken nearly simultaneously with the last light through the SVST on August 14, 2000. Top: G band, 1 nm FWHM filter centered at $\lambda = 430.5$ nm, 10-bit camera, 12 ms exposure. Bottom: CN band, 1 nm FWHM filter centered at $\lambda = 387.4$ nm, 8-bit camera, 50 ms exposure. The second image is less sharp, primarily due to the longer exposure, but the solar scene is the same in the two images.

6. Conclusion

When the standard fluxtube models are combined with the standard assumptions under which they were constructed, the computed and observed G-band bright point contrasts agree well. The G band thanks its increased contrast to enhanced dissociation of CH within the fluxtubes, increasing the visibility of the hot subsurface tube walls. The CN band around $\lambda = 387.4$ nm displays magnetic elements in comparable fashion at 1 nm bandwidth.

This agreement does not discriminate between the three options in Fig. 2. It only confirms that the standard models reproduce many spectral diagnostics well when LTE and the model geometry are similarly assumed in the diagnostic formation modeling.

Acknowledgements. We are indebted to Sami Solanki and Carine Briand for fluxtube models and model-processing codes. R.J. Rutten thanks the organizers for an excellent workshop and acknowledges travel support from the Leids Kerkhoven Bosscha Fonds. The SVST was operated by the Royal Swedish Academy of Sciences at the Spanish Observatorio del Roque de los Muchachos of the Instituto de Astrofísica de Canarias. The Utrecht–Stockholm collaboration is part of the EC–TMR European Solar Magnetometry Network (ESMN).

References

Auffret H., Muller R., 1991, A&A 246, 264
Bellot Rubio L. R., Ruiz Cobo B., Collados M., 1998, ApJ 506, 805
Berger T. E., Löfdahl M. G., Shine R. A., Title A. M., 1998a, ApJ 506, 439
Berger T. E., Löfdahl M. G., Shine R. S., Title A. M., 1998b, ApJ 495, 973
Berger T. E., Schrijver C. J., Shine R. A., Tarbell T. D., Title A. M., Scharmer G., 1995, ApJ 454, 531
Berger T. E., Title A. M., 1996, ApJ 463, 365
Briand C., Solanki S. K., 1995, A&A 299, 596
Bruls J. H. M. J., Solanki S. K., 1993, A&A 273, 293
Bünte M., Solanki S. K., Steiner O., 1993, A&A 268, 736
Dermendjev V. N., Muller R., Madjarska M. S., 1994, Solar Phys. 155, 45
Fraunhofer J., 1817, Denkschriften der Münch. Akad. der Wissenschaften 5, 193
Grossmann-Doerth U., Schüssler M., Steiner O., 1998, A&A 337, 928
Kiselman D., Rutten R. J., Plez B., 2001, in P. Brekke, B. Fleck, J. B. Gurman (eds.), Recent Insights into the Physics of the Sun and Heliosphere, Procs. IAU Symposium 203, ASP Conf. Ser., Vol. 200, in press
Leka K. D., Steiner O., Grossmann-Doerth U., 1999, in American Astronomical Society Meeting, Vol. 194, p. 5507
Liu S. Y., Sheeley N. R., 1971, Solar Phys. 20, 282
Löfdahl M. G., Berger T. E., Shine R. S., Title A. M., 1998, ApJ 495, 965
Löfdahl M. G., Scharmer G. B., 1994, A&AS 107, 243
Maltby P., Avrett E. H., Carlsson M., Kjeldseth-Moe O., Kurucz R. L., Loeser R., 1986, ApJ 306, 284
Moity J., Muller R., Dollfus A., Montagne M., Vigneau J., 1999, in B. Schmieder, A. Hofmann, J. Staude (eds.), Magnetic Fields and Oscillations, Procs. Third Adv. Solar Physics Euroconf., ASP Conf. Ser. 184, p. 211
Muller R., 1994, in R. J. Rutten, C. J. Schrijver (eds.), Solar Surface Magnetism, NATO ASI Series C Vol. 433, Kluwer, Dordrecht, p. 55
Muller R., Hulot J. C., Roudier T., 1989, Solar Phys. 119, 229
Muller R., Roudier T., 1992, Solar Phys. 141, 27
Muller R., Roudier T., 1994, Solar Phys. 152, 131
Muller R., Roudier T., Vigneau J., Auffret H., 1994, A&A 283, 232
Roudier T., Espagnet O., Muller R., Vigneau J., 1994, A&A 287, 982
Ruiz Cobo B., Del Toro Iniesta J. C., 1992, ApJ 398, 375
Rutten R. J., 1999, in B. Schmieder, A. Hofmann, J. Staude (eds.), Magnetic Fields and Oscillations, Procs. Third Adv. in Solar Physics Euroconf., ASP Conf. Ser., Vol. 184, p. 181
Rutten R. J., Uitenbroek H., 1991, Solar Phys. 134, 15
Sánchez Almeida J., 1997, ApJ 491, 993
Sánchez Almeida J., Landi Degl'Innocenti E., Martínez Pillet V., Lites B. W., 1996, ApJ 466, 537
Sánchez Almeida J., Lites B. W., 2000, ApJ 532, 1215
Schrijver C. J., Zwaan C., 2000, Solar and Stellar Magnetic Activity, Cambridge Univ. Press, Cambridge, UK
Solanki S., Steiner O., Uitenbroek H., 1991, A&A 250, 220
Solanki S. K., 1986, A&A 168, 311
Solanki S. K., Brigljevic V., 1992, A&A 262, L29
Solanki S. K., Stenflo J. O., 1985, A&A 148, 123
Spruit H. C., 1974, Solar Phys. 34, 277
Spruit H. C., 1977, Magnetic flux tubes and transport of heat in the convection zone of the Sun, PhD thesis, Utrecht University

Spruit H. C., 1979, Solar Phys. 61, 363
Spruit H. C., 1981, in S. D. Jordan (ed.), The Sun as a Star, NASA-CNRS Monograph series on nonthermal phenomena in stellar atmospheres, NASA SP-450, p. 385
Spruit H. C., Zwaan C., 1981, Solar Phys. 70, 207
Steiner O., Grossmann-Doerth U., Knölker M., Schüssler M., 1998, ApJ 495, 468
Stuik R., Bruls J. H. M. J., Rutten R. J., 1997, A&A 322, 911
Title A. M., Berger T. E., 1996, ApJ 463, 797
van Ballegooijen A. A., 1985, in H. U. Schmidt (ed.), Theoretical Problems in High Resolution Solar Physics, Procs. Solar Opt. Tel. Workshop, Max Planck Inst. Astrophysik, München, p. 167